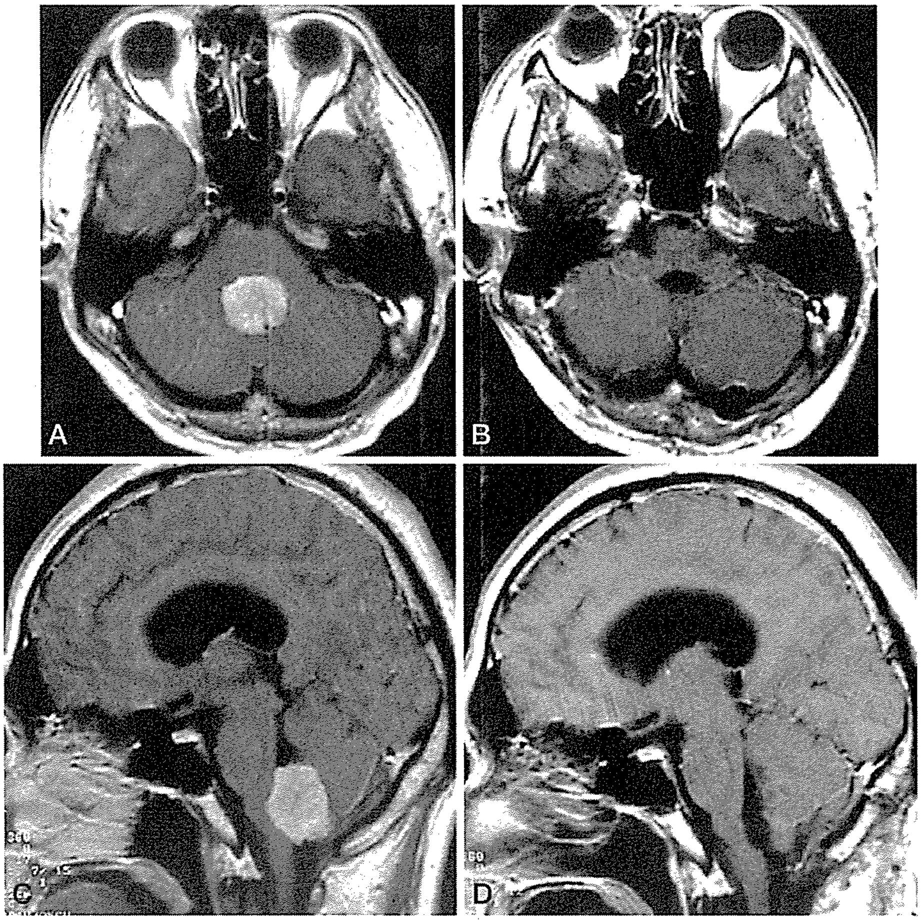

Fig. 4 Case 4, a 37-year-old male with choroid plexus papilloma. Magnetic resonance (MR) imaging with gadolinium (**A**: axial, **C**: sagittal) showed an enhanced mass in the fourth ventricle. The tumor was totally resected (**B**: axial, **D**: sagittal) and he remained in good condition with no deficit.

り初回手術で部分摘出に終わった29歳女性の症例（Case 3）においてのみ，術後に局所60 Gyの照射とACNUによる化学療法を追加した．この症例以外のCPPに対しては補助療法を行っていない．

これら7症例の観察期間は21～140カ月で平均63.0カ月であった．予後については，生存例は7例中6例で，死亡例は1例であった．死亡例は脳幹に浸潤した第4脳室発生のCPPの症例（Case 3）で，初期治療後4年で再発を生じたため2回の追加切除を行ったが，脳幹部病変の増大と頸髄への播種病変により81カ月で窒息死している．後遺障害としては，側脳室発生の2カ月男児のCPC例（Case 5）が発育遅延を来したことと，延髄から上位頸髄に浸潤した領域を全摘出した3歳男児のCPC例（Case 6）が術前からの嚥下障害が残存していることが挙げられる．これら以外の4症例については神経学的脱落症状のない状態で生存中である．

Ⅲ. 考　察

CPTは全頭蓋内腫瘍の0.4～1.0%程度と稀な腫瘍である[3,15,22,24]．男女比については，一般にCPPでは性差はないとされるが[13,15]，CPCでは89%が男性だったとする報告もある[15]．好発部位は小児では側脳室，成人では第4脳室が多いが

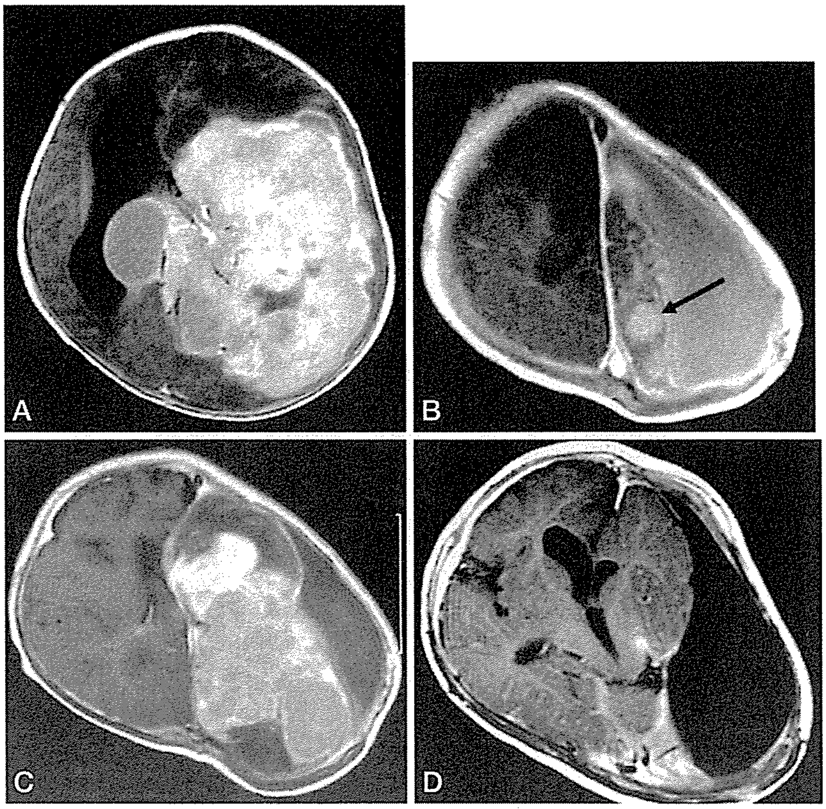

Fig. 5 Case 5, a 2-month-old boy with choroid plexus carcinoma. Magnetic resonance (MR) imaging with gadolinium showed an enhanced mass in the left lateral ventricle (**A**). The tumor was resected subtotally at the first surgery, leaving a small enhanced mass in the parietal region (**arrow**) with clots in the ventricles and the subdural space (**B**). Five months after the first surgery, the residual tumor had enlarged (**C**). The residual tumor was totally removed at the second operation with intraoperative radiation (**D**). Thereafter, ventriculo-peritoneal shunting was necessary for hydrocephalus. Mental retardation and symptomatic epilepsy persisted, but he was in good condition 10 years after the surgery.

[25]，側脳室発生例では悪性は少ないとされる[20]．好発年齢は小児に多く[3,8,11,25]，217文献566例をレビューしたWolffらの論文では，診断時の平均年齢は3.5歳であった[25]．当施設の症例では7例中，成人例が4例とこれまでの報告と比べて成人例が多い．

CPTでは手術摘出度が予後(合併症率，死亡率)に相関しており，全摘出こそが最重要とされている[3,10,15,16,25]．特にCPCにおいて手術の役割が大きいとする意見もあり[17]，CPCでは全摘例では亜全摘例と比較して予後が明らかに良好である[2,8,10]．手術摘出度については，当施設の症例では組織型の違いによる差は認めなかった．組織の悪性度と手術摘出度ついては，われわれ同様に相関しなかったという意見もあるが[16]，栄養血管の豊富さや腫瘍の大きさ，浸潤傾向などからCPCのほうがCPPよりも全摘が困難とする報告もある[8,18]．

予後を考えると可及的摘出がまず第一だが，病変が第4脳室に存在する場合は，腫瘍の脳幹部への浸潤が全摘を困難なものにしている．実際，当施設での症例を検討すると，病変が側脳室あるいは第3脳室に存在する症例では最終的には全摘出が可能だったが，第4脳室に存在する症例では5例中3例が亜全摘にとどまっている．これら3例のうち1例では再発を繰り返し，最終的に脳幹病変の増大と頸髄への播種により死亡している(Case 3)．一方，全摘した2例のうちの1例(Case 6)では，術前から認められていた嚥下障害が術後も残存している．脳幹部病変に対する術後の後遺症としては，橋に発生したCPPで術後に片麻痺が残った症例[19]や，第4脳室発生のCPPの摘出術後に構音障害，嚥下障害が残存したという報告がある[4]．この領域の病変では手術による全摘出を目指す一方で，機能温存のためには摘出操作をどこでとどめるべきかというジレンマがあるた

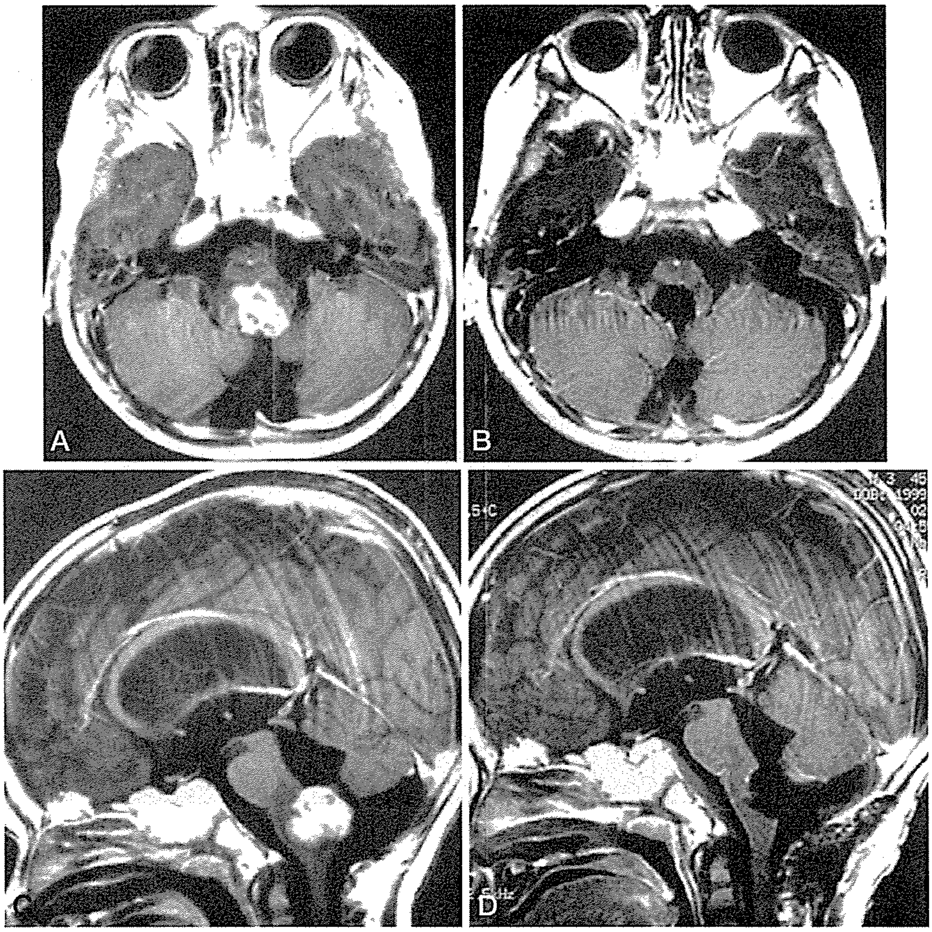

Fig. 6 Case 6, a 3-year-old boy with choroid plexus carcinoma. The patient had dysphagia at the first visit to our hospital. Magnetic resonance (MR) imaging with gadolinium (**A**: axial, **C**: sagittal) showed an enhanced mass in the fourth ventricle. Endoscopic third ventriculostomy was performed for hydrocephalus before resection of the tumor. The tumor was resected totally at surgery (**B**: axial, **D**: sagittal). He received radiation as adjuvant therapy.

め，治療戦略を立てるのが難しい．

組織学的悪性度の高いCPCはCPTの10～25%を占めるといわれており[2,20]，予後はCPPよりも不良とされる[24]．特に小児例では予後が不良である[3,5]．5年生存率についてもさまざまな報告があるが，CPPでは81～100%であるのに対し，CPCでは26～50%と明らかに成績が悪い[2,6,8,13,18,25]．過去にCPCの長期生存例の報告もなされているものの[11]，CPCは一般には予後不良である．しかしながら，以前はCPCの平均生存期間が9カ月程度だったのに対し[5]，最近の報告では平均生存期間が48カ月にまで延長している[17]．診断技術，手術，補助療法のいずれの進歩が理由かは不明だが，手術の占める要素が大きいのは確かである．CPCの5年生存率は26%だったとするBergerらの報告でも，全摘例に限っていえば5年生存率は86%にまで上昇している[2]．この報告ではCPCは手術による摘出度こそが予後因子であり，年齢，性別，初発症状から診断までの期間，場所，大きさ，補助療法などと予後は相関しないとしている[2]．当科の症例をみても2カ月男児の症例は初回亜全摘後に急速に残存腫瘍

Fig. 7 Case 7, a 25-year-old female with choroid plexus carcinoma. Magnetic resonance (MR) imaging with gadolinium (**A**: axial, **C**: sagittal) showed an enhanced mass in the fourth ventricle. The tumor was subtotally resected (**B**: axial, **D**: sagittal), followed by radiation and chemotherapy to the residual tumor (**arrows**).

が拡大したため再手術により全摘したところ，術中照射と化学療法を追加した効果もあるものの，その後10年間は再発を生じておらず，全摘の重要性が示唆される[14]．

術後の補助療法については確固たるエビデンスはないが，CPPとCPCでは治療方針は異なってくる．CPPの術後照射についての意見は分かれるが，初回手術で全摘，亜全摘いずれの場合でも放射線治療は予後を改善させてはいない[13,16]．しかし再発例については，可及的摘出後の放射線療法は適応だろうとされている[16]．一方，CPCに対しては術後の放射線療法が予後と相関しており，全摘出後でも放射線療法を受けるべきとする意見がある[24,25]．Wolffらによると，全摘出後のCPCの照射群では5年生存率が68%なのに対し，非照射群では16%で[24]，照射が可能な年齢であればCPCに対しては放射線療法を積極的に追加するべきであろう[24]．照射は年長児以上に限られるが，髄液播種などの再発様式などを考慮すると全脳全脊髄照射が推奨されている[2,8,17]．

CPPに対する化学療法については，エビデンスはないとされている．全摘後の治療成績がよいことも考慮すると，CPPの初回手術後は補助療法を行わずにまず経過観察がよいと考えられる

Table Clinical summary of 7 patients with tumors of the choroid plexus

Case	Age	Gender	Location	Surgery	Shunt	Pathology	Radiation	Chemotherapy	Prognosis	Survival period (months)
1	4m	F	3rd ventricle	total	SPS (post-ope)	CPP	none	none	no deficit	21
2	28	M	4th ventricle	subtotal	none	CPP	none	none	no deficit	104
3	29	F	4th ventricle	subtotal, partial (2nd), subtotal (3rd)	VPS (post-ope)	CPP	L60 Gy	ACNU	dead (respiratory disturbance)	81
4	37	M	4th ventricle	total	none	CPP	none	none	no deficit	32
5	2m	M	lateral ventricle	subtotal, total (2nd)	VPS (post-ope)	CPC	IOR10 Gy	VCR, MTX	mental retardation, epilepsy	140
6	3	M	4th ventricle	total	ETV (pre-ope)	CPC	WB&WS24 Gy, L26 Gy	none	dysphagia	34
7	25	F	4th ventricle	subtotal	none	CPC	WB&WS30 Gy, L24 Gy	ACNU	no deficit	29

m: month, **F**: female, **M**: male, **CPP**: choroid plexus papilloma, **CPC**: choroid plexus carcinoma, **L**: local, **IOR**: intraoperative radiation, **WB**: whole brain, **WS**: whole spine **VPS**: ventriculo-peritoneal shunt, **ETV**: endoscopic third ventriculostomy, **SPS**: subdural-peritoneal shunt

[22,25]．しかし，最近の報告ではCPPの再発，脊髄播種後に放射線療法に加えてCCNUを併用したところ腫瘍の消退の効果があったとしており[23]，CPPの再発時におけるCCNU投与は有用かもしれない．

一方，CPCに対する化学療法の効果は不明とする意見もあるが[25]，化学療法を推奨する意見のほうが多い[7]．投与方法については，術前に行う場合と術後に追加する場合のいずれも報告されている．術前の化学療法についての報告では，腫瘍容積を縮小したり腫瘍の栄養血管を減じるため，全摘を目指すうえで効果的としている[1,7]．Souweidaneらは15カ月のCPCの女児に対して，etoposide，cyclophosphamide，vincristine，cisplatinなどを用いて術前に化学療法を行ったところ，腫瘍容積を29.5%減じることができ，全摘を可能にしたと報告している[21]．CPCに対する術後の化学療法については，全摘されていれば必ずしも必要としないとする意見もあるが[10]，全摘後でも術後に放射線療法とともに化学療法を考慮すべきという意見もある[22]．亜全摘後の化学療法では11例中4例でCR（complete recovery）という報告もあり，CPCに対する術後化学療法の有用性を示している[2]．また，部分摘出術後にcarboplatin，doxorubicin，methotrexateによる化学療法を追加したところ完全寛解を得られたという報告もある[9]．これらの結果より，少なくともCPCに対しては術前，術後を問わず積極的な化学療法が有用と考えられる．予後不良という観点からも手術摘出度に関係なく化学療法を行うべきという意見もある[2]．当施設でのCPCの症例では亜全摘に終わった2例で化学療法を追加しているが，全摘例の1例と合わせてすべて生存中である．ただし，化学療法の内容に関しては確立されたものはなく，今後の検討が望まれる．

当院での経験と過去の文献を検討した結果，CPTにおいて最大の予後因子はやはり手術による摘出度であるといえる．CPPは基本的に良性腫瘍なので全摘がなされていれば補助療法は追加せず，亜全摘でも経過観察を行い，再発時（再増大時）に手術による可及的摘出と補助療法を追加する方針がよいと考えられる．また組織学的により悪性度の高いCPCでも可及的摘出は大前提ではあるが，術前化学療法も含めて積極的に補助療法を考慮すべきで，全摘がなされた場合でも術後の放射線療法，化学療法の追加は必要であろう．全摘を妨げる因子としては腫瘍の部位，浸潤度が影響してくるが，特に第4脳室病変では脳幹部への浸潤が全摘を阻むことになるため，症例ごとに機能温存と生命予後との関係を術前に十分に説明

しておく必要があるだろう．

文 献

1) 荒木加寿美，青木友和，高橋 潤，野崎和彦，永田泉，菊池晴彦，横山瑞香，服部春夫，秋山祐一，久保田優，横溝 大：Choroid plexus carcinoma の 1 例. No Shinkei Geka **25**：853-857, 1997
2) Berger C, Thiesse P, Lellouch-Tubiana A, Kalifa C, Pierre-Kahn A, Bouffet E：Choroid plexus carcinomas in childhood：clinical features and prognostic factors. Neurosurgery **42**：470-475, 1998
3) Boyd MC, Steinbok P：Choroid plexus tumors：problems in diagnosis and management. J Neurosurg **66**：800-805, 1987
4) Cornwell PL, Murdoch BE, Ward EC, Morgan A：Dysarthria and dysphagia following treatment for a fourth ventricle choroid plexus papilloma. J Clin Neurosci **10**：506-512, 2003
5) Dohrmann GJ, Collias JC：Choroid plexus carcinoma. Case report. J Neurosurg **43**：225-232, 1975
6) Due-Tonnessen B, Helseth E, Skullerud K, Lundar T：Choroid plexus tumors in children and young adults：report of 16 consecutive cases. Childs Nerv Syst **17**：252-256, 2001
7) Duffner PK, Kun LE, Burger PC, Horowitz ME, Cohen ME, Sanford RA, Krischer JP, Mulhern RK, James HE, Rekate HL, et al：Postoperative chemotherapy and delayed radiation in infants and very young children with choroid plexus carcinomas. The Pediatric Oncology Group. Pediatr Neurosurg **22**：189-196, 1995
8) Ellenbogen RG, Winston KR, Kupsky WJ：Tumors of the choroid plexus in children. Neurosurgery **25**：327-335, 1989
9) Fiorillo A, Maggi G, Cirillo S, Migliorati R, Buffardi F, Alfieri E, Sabbatino MS, D'Amico A, Del Basso De Caro ML：Efficacy of sequential chemotherapy including methotrexate and doxorubicin in an infant with partially resected choroid plexus carcinoma. Pediatr Neurosurg **38**：21-26, 2003
10) Fitzpatrick LK, Aronson LJ, Cohen KJ：Is there a requirement for adjuvant therapy for choroid plexus carcinoma that has been completely resected? J Neurooncol **57**：123-126, 2002
11) Hawkins JC 3rd：Treatment of choroid plexus papillomas in children：a brief analysis of twenty years' experience. Neurosurgery **6**：380-384, 1980
12) Kimura M, Takayasu M, Suzuki Y, Negoro M, Nagasaka T, Nakashima N, Sugita K：Primary choroid plexus papilloma located in the suprasellar region：case report. Neurosurgery **31**：563-566, 1992
13) Krishnan S, Brown PD, Scheithauer BW, Ebersold MJ, Hammack JE, Buckner JC：Choroid plexus papillomas：a single institutional experience. J Neurooncol **68**：49-55, 2004
14) Kumabe T, Tominaga T, Kondo T, Yoshimoto T, Kayama T：Intraoperative radiation therapy and chemotherapy for huge choroid plexus carcinoma in an infant. Neurol Med Chir (Tokyo) **36**：179-184, 1996
15) McEvoy AW, Harding BN, Phipps KP, Ellison DW, Elsmore AJ, Thompson D, Harkness W, Hayward RD：Management of choroid plexus tumors in children：20 years experience at a single neurosurgical centre. Pediatr Neurosurg **32**：192-199, 2000
16) McGirr SJ, Ebersold MJ, Scheithauer BW, Quast LM, Shaw EG：Choroid plexus papillomas：long-term follow-up results in a surgically treated series. J Neurosurg **69**：843-849, 1988
17) Packer RJ, Perilongo G, Johnson D, Sutton LN, Vezina G, Zimmermann RA, Ryan J, Reaman G, Schut L：Choroid plexus carcinoma of childhood. Cancer **69**：580-585, 1992
18) Pencalet P, Sainte-Rose C, Lellouch-Tubiana A, Kalifa C, Brunelle F, Sgouros S, Meyer P, Cinalli G, Zerah M, Pierre-Kahn A, Renier D：Papillomas and carcinomas of the choroid plexus in children. J Neurosurg **88**：521-528, 1998
19) Pillai A, Rajeev K, Chandi S, Unnikrishnan M：Intrinsic brainstem choroid plexus papilloma. Case report. J Neurosurg **100**：1076-1078, 2004
20) Raimondi AJ, Gutierrez FA：Diagnosis and surgical treatment of choroid plexus papillomas. Childs Brain **1**：81-115, 1975
21) Souweidane MM, Johnson JH Jr, Lis E：Volumetric reduction of a choroid plexus carcinoma using preoperative chemotherapy. J Neurooncol **43**：167-171, 1999
22) Strojan P, Popovic M, Surlan K, Jereb B：Choroid plexus tumors：a review of 28-year experience. Neoplasma **51**：306-312, 2004
23) Valencak J, Dietrich W, Raderer M, Dieckmann K, Prayer D, Hainfellner JA, Marosi C：Evidence of therapeutic efficacy of CCNU in recurrent choroid plexus papilloma. J Neurooncol **49**：263-268, 2000
24) Wolff JE, Sajedi M, Coppes MJ, Anderson RA, Egeler RM：Radiation therapy and survival in choroid plexus carcinoma. Lancet **353**：2126, 1999
25) Wolff JE, Sajedi M, Brant R, Coppes MJ, Egeler RM：Choroid plexus tumours. Br J Cancer **87**：1086-1091, 2002

J Neurosurg 106:90–98, 2007

Visualization of the frontotemporal language fibers by tractography combined with functional magnetic resonance imaging and magnetoencephalography

KYOUSUKE KAMADA, M.D.,[1] TOMOKI TODO, M.D.,[1] YOSHITAKA MASUTANI, PH.D.,[2] SHIGEKI AOKI, M.D.,[2] KENJI INO, R.T.,[2] AKIO MORITA, M.D.,[1] AND NOBUHITO SAITO, M.D.[1]

Departments of [1]Neurosurgery and [2]Radiology, Faculty of Medicine, The University of Tokyo, Japan

Object. There is continuous interest in the monitoring of language function during tumor resection around the frontotemporal regions of the dominant hemisphere. The aim of this study was to visualize language-related subcortical connections, such as the arcuate fasciculus (AF) by diffusion tensor (DT) imaging–based tractography.

Methods. Twenty-two patients with brain lesions adjacent to the AF in the frontotemporal regions of the dominant hemisphere were studied. The AF tractography was accomplished by placing initiation and termination sites (seed and target points) in the frontal and temporal regions, which were functionally identified by using functional magnetic resonance (fMR) imaging in conjunction with a verb generation task and magnetoencephalography (MEG) in conjunction with a reading task. The combination of fMR imaging and MEG data clearly demonstrated the hemispheric dominance of language functions, which was confirmed by an intracranial amobarbital test (Wada procedure). In all 22 patients, the authors were able to consistently visualize the AF by DT imaging–based tractography, using the functionally identified seed and target points and a fractional anisotropy value of 0.16. In two of 22 cases investigated, the functional information, including the results of AF tractography, fMR imaging, and MEG, was imported to a neuronavigation system and was validated by bipolar electric stimulation of the cortical and subcortical areas during awake surgery. The cortical stimulation to the gyrus that included the area of activation identified in fMR imaging with the language task evoked speech arrest, while the subcortical stimulation close to the AF reproducibly caused paranomia without speech arrest. Postoperative AF tractography showed that the distances between the stimulus points and the AF were within 6 mm.

Conclusions. The combination of these techniques facilitated accurate identification of the location of the AF and verification of the language fibers.

KEY WORDS • arcuate fasciculus • subcortical stimulation • functional magnetic resonance imaging • language • magnetoencephalography • tractography

TUMOR resection in the frontotemporal regions of the dominant hemisphere entails a high risk of neurological consequences to language functions. It is essential to preserve the subcortical connections related to these language functions in addition to sparing eloquent cortices from injury. Several groups have proposed electrical subcortical stimulation during awake surgery as a reliable way to identify the eloquent subcortical connections.[6,7,11] However, there are several difficulties associated with this procedure, including the need to identify, for optimal stimulus points, the need for patients' cooperation and certain risks related to anesthesia. It is therefore desirable to quickly and accurately find the eloquent fibers of language functions within the limited operation time.

Recent progress in functional brain imaging has allowed the visualization of white matter connections in addition to the cortical distribution of language functions.[9,17,18] Fiber tracking processes (tractography) allow visualization of the major axonal fascicles of interest through calculation of the DT of each pixel.[1,14] Recently, several groups have succeeded in integrating DT imaging–based tractography of the corticospinal tract and the optic radiation into neuronavigation systems and have verified the integrated fibers by using electrophysiological techniques.[2,11]

The AF allows the connection between two essential epicenters of the language network—the IFG and the dorsolateral PFCs—and the posterior temporal region within the dominant hemisphere. It is very difficult to extract anisotropic components of the AF from DT imaging data because there are no anatomical landmarks for the initiation of tractography, and other subcortical fibers, such as the superior and inferior longitudinal fascicles and the corticospinal tract, were densely packed together with the AF in the frontotemporal region.

We recently reported the use of the combination of fMR

Abbreviations used in this paper: AF = arcuate fasciculus; DT = diffusion tensor; fMR = functional magnetic resonance; GBM = glioblastoma multiforme; IFG = inferior frontal gyrus; MEG = magnetoencephalography; MFG = middle frontal gyrus; MTG = middle temporal gyrus; PFC = prefrontal cortex; SMG = supramarginal gyrus; STG = superior temporal gyrus.

imaging and MEG to noninvasively detect the cortical areas of specific language functions.[9,10] In our study, we were able to clearly identify the expressive language area using fMR imaging in combination with a verb generation task, whereas MEG in combination with a reading task successfully depicted the receptive language function. By combining the advantages of the two approaches, we established a reliable method to identify the areas involved in global language functions. We have applied these noninvasive mapping techniques to identify the initiation and terminal sites (seed and target points) for AF tractography.

In the current study, we investigated 22 cases of brain lesions located in the dominant frontotemporal area and successfully visualized the spatial relationships between the AF and the lesions. In two of the 22 cases, the functional information, including the results of AF tractography, fMR imaging, and MEG, were imported to a neuronavigation system (functional neuronavigation), and the findings were validated using cortical and subcortical stimulation during awake surgery in these two patients. In this paper we describe the usefulness of DT imaging–based tractography for localizing language functions and demonstrate its reliability using subcortical mapping in two of the 22 cases studied.

Clinical Material and Methods

Patient Population

We studied 22 patients harboring an intraaxial tumor in the frontotemporal language area of the dominant hemisphere. All patients had little impairment of expressive or receptive language functions, except for dysarthria and hemiparesis, and underwent the intracranial amobarbital procedure (Wada test) to identify the language dominance. Because two of the patients had a lesion that partially involved the AF, we decided that they were candidates for awake surgery to spare the eloquent subcortical connections of language functions.

This study was approved by the institutional review board, and written informed consent was obtained from each subject before participation in the studies.

Visualization of the Language Networks

To place the seed and target points for AF tractography, we needed to localize the cortical language functions using fMR imaging and MEG. Details of the noninvasive cortical mapping have been reported elsewhere.[10]

Magnetic Resonance Imaging Protocols

All MR imaging was performed using a 1.5-tesla whole-body unit with echo planar capabilities and a standard whole-head transmitter–receiver coil (Vision, Siemens: Signa Echospeed, General Electric Medical Systems). During the experiments, foam cushions were used to immobilize the patient's head.

Functional MR Imaging With a Language Task

Functional MR imaging was performed with a T_2*-weighted echo planar imaging sequence (TE 62 msec; TR 114 msec; flip angle 90°; slice thickness 4 mm; slice gap 2 mm; field of view 260 mm; matrix 64 × 128; 14 slices). Each fMR imaging session consisted of three dummy image volumes, three activation periods, and four baseline (rest) periods. During each period, five echo planar imaging volumes were collected, yielding a total of 38 imaging volumes. Each patient was asked to silently generate a verb related to each acoustically presented noun. The interstimulus intervals ranged from 1600 to 2400 msec during the active periods. Reverse playback of the sound files was used to eliminate primary auditory activation for the rest period, using exactly the same interstimulus intervals as the active condition. The auditory stimuli were delivered binaurally via two 5-m-long plastic tubes terminating at headphones.

After acquiring the data, we used a motion detection program (MEDx, Medical Numerics) to identify and eliminate fMR imaging sessions containing motion artifact of more than 25% of the pixel size. After applying a gaussian spatial filter (7 mm in half width), we calculated functional activation maps by estimating the Z scores between the rest and activation periods, using Dr. View software (Asahi Kasei). Clusters with a Z score greater than 2.2 were accepted as indicating real activation. The result of each fMRI session was coregistered to 3D T_1-weighted MR images of each subject's head, maximizing the mutual information of the data sets with the affine transformation.[5]

Magnetoencephalography With a Language Task

The MEG signals were recorded with a 204-channel biomagnetometer (VectorView, Neuromag) in a magnetically shielded room. One hundred fifty words consisting of three Japanese letters were visually presented with a 300-msec exposure time and interstimulus intervals ranging from 2800 to 3200 msec during the MEG recording sessions, and the patients were asked to categorize the presented word as abstract or concrete. The averaged magnetic signals were digitally filtered between 0.1 and 30 Hz and obvious MEG deflections were visually identified on the basis of root mean squared fields of more than 10 sensors. Locations and moments of equivalent current dipoles were calculated every 2 msec from 250 to 600 msec after the stimulus onsets, using the single equivalent dipole model. Only dipoles with a correlation value of more than 0.85 were accepted. These dipoles were superimposed onto 3D MR images according to anatomical fiduciary landmarks.

Thus we obtained functional 3D MR images containing fMR imaging and MEG results and showing the cortical distribution of the language functions.

Diffusion Tensor Imaging–Based AF Tractography

Diffusion Tensor Imaging

All DT imaging was performed using a single-shot spin echo–echo planar sequence with an echo time of 66.4 msecs and a repetition time of 13000 msecs. Fifty-five interleaved, gapless, 3-mm-thick axial images were acquired in order to cover the entire brain. A field of view of 24 × 24 cm and a matrix of 128 × 128 interpolated to 256 × 256 were used. Diffusion gradients were applied in 15 noncollinear independent axes using a b value of 1000 seconds/mm^2 as the peak diffusion gradient. Non–diffusion-weighted images (T_2-weighted images) were also obtained with a b value of 0 seconds/mm^2. Realignment of these 15 DT imaging sets and compensation for eddy-current–induced morphing were performed on the basis of a T_2-weighted echo planar imaging set (b = 0) on an equipped workstation (Advantage Workstation 4.0, General Electric).[15]

Diffusion Tensor Calculation and DT Imaging–Based Tractography

The DT imaging data sets were analyzed by using freeware for diffusion tensor analysis and fiber tracking (Volume-One and dTV; URL: http://volume-one.org).[14] Interpolation along the z axis was also applied to obtain isotropic data (with a voxel size of 0.94 × 0.94 × 0.94 mm). The software determined six elements of the symmetric 3 × 3 matrix of the diffusion tensor at each voxel by least-square fitting, and the diffusion tensor was diagonalized to obtain three eigenvalues and three eigenvectors. The eigenvector ($e1$) associated with the largest eigenvalue ($\lambda 1$) was assumed to represent the local fiber direction. Anisotropy maps were obtained using orientation-independent fractional anisotropy. Coregistration between T_2-weighted echo planar images including the DT imaging–based tractography and functional 3D MR images was performed based on the maximization of mutual information by affine transformation.[5,15]

We determined the seed point for AF tractography on the functional 3D MR images of the frontal lobe so as to include most of the area of activation identified on fMR imaging using the language task. Similarly, the target was drawn on the ipsilataral superior temporal region, where the MEG language study dipoles were clustered. Diffusion tensor imaging–based tractography was initiated from the seed point from which lines were propagated in both anterograde and retrograde directions according to $e1$ at each pixel. Only the trajectories of the AF passing through both the seed and target points were retained for the analysis. When a pixel with an fractional anisotropy value lower than 0.16 was reached, the tracking process was terminated.

Two patients (Cases 21 and 22), who had lesions that partially involved the AF, underwent surgery with local anesthesia (awake surgery) so that functional cortical and subcortical mapping could be performed using electrical stimulation. For this procedure, we used additional processes as described in the following section.

Voxelization, Image Registration, Data Fusion, and Functional Neuronavigation

After AF fiber tracking, voxels containing tract fibers were marked with volume data, using the same matrix size is in DT imaging—in other words, voxelization of the tracking lines was performed. Because of the coregistration, the voxelized AF was in the same coordinate system of the T_2-weighted echo planar imaging data. Finally, the voxelized AF and the functional 3D MR images were simply fused and resliced using the DICOM (Digital Imaging and Communications in Medicine) format according to the original anatomical 3D MR imaging header information. After all these processes were completed, the results were visually evaluated by at least two radiologists and one neurosurgeon.

The resliced functional 3D MR imaging data, including the AF tractography data, was transferred to a neuronavigation system (Stealthstation; Medtronic Sofamor Danek). The neuronavigation system software was used to segment the functional information by setting the signal thresholds and color the areas identified by AF tractography, areas of fMR imaging activation, and MEG dipoles as yellow, red and blue, respectively. In this manner we performed functional neuronavigation.

Cortical and Subcortical Mapping

A bipolar electrode with tips spaced 5 mm apart and delivering a biphasic current with a pulse frequency of 50 Hz and a single pulse phase duration of 1 msec (Ojemann Cortical Stimulator; Unique Medical) was applied to the brain of awake patients.

Cortical mapping was performed after the tumor and sulci/gyri had been identified using functional neuronavigation and ultrasonography. Motor mapping was performed first to find the appropriate stimulus intensity. The specific current intensity used for each patient was determined by progressively increasing the amplitude from a baseline of 4 mA, until a motor response (inhibition of voluntary hand movement by muscle contraction) was elicited, with 10 mA as the upper limit, and the goal of avoiding the generation of seizures. Once the motor mapping threshold was defined, the same intensity was used for both cortical and subcortical mapping of language functions. We systematically used simple language tasks, such as spontaneous speech, picture naming, and auditory comprehension, and stimulus points were determined by functional neuronavigation.

The patients were first asked to repeatedly speak the sentence, "The weather is good today," and the cortical regions in which cortical stimulation caused speech arrest or dysarthria were marked with sterilized tags. For the naming task, we showed the patients 20 different pictures, which were simple and easy to recognize during awake surgery, and observed the degree of speech arrest or paranomia caused by cortical and subcortical stimulation. During the auditory comprehension task, the patients were asked to follow simple verbal commands, such as requests to shake their hands, move their fingers, and open their mouths.

We removed the lesions, alternating resection and subcortical stimulation. The patients were asked to continue to speak a sentence or name an object when the resection approached the AF. We pursued resection in each case until we encountered eloquent pathways around the surgical cavity, as identified by functional neuronavigation and subcortical stimulation.

Results

Functional MR Imaging With a Verb Generation Task

The verb generation task was completed by and useful fMR imaging data was obtained from all 22 patients. Pixels activated during the verb generation task were clustered mainly in the IFG, MFG, dorsolateral PFC, and supplementary motor area. Activation in the IFG and MFG was significantly lateralized and therefore served as a good indicator for the dominant hemisphere in all patients (Fig. 1A). We found that the left hemisphere was dominant for expressive language function in 19 patients and the right in three patients (Figs. 1A and 2A). Functional MR imaging demonstrated activation in the suspected dominant hemisphere as

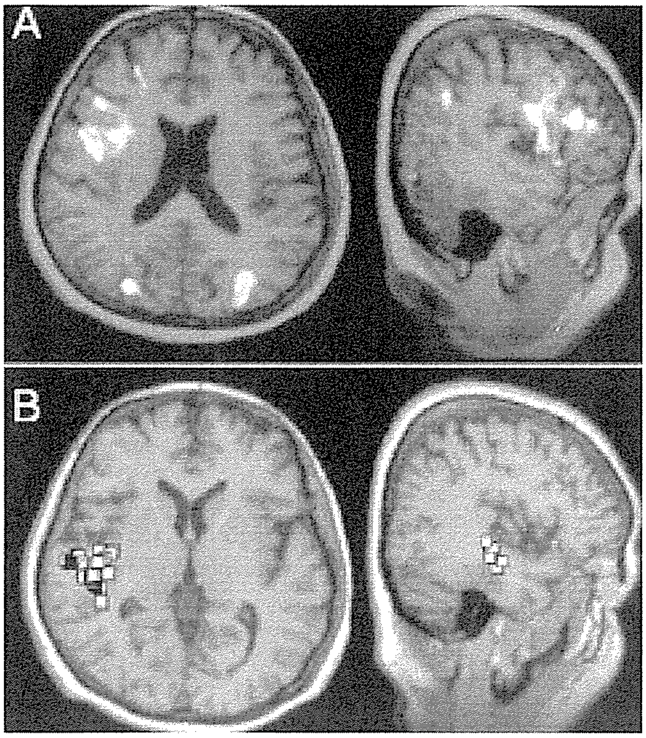

FIG. 1. Case 21. A right frontal lobe tumor in a 61-year-old, left-handed woman. A: Functional MR images obtained during a language task showing activation predominantly in the right IFG and the inferior part of the MFG. B: Magnetoencephalography source localizations obtained during a language task, superimposed on MR images, showing dipole clusters predominantly in the right STG and MTG. The left and right hemispheres contained 37 and 127 dipoles, respectively.

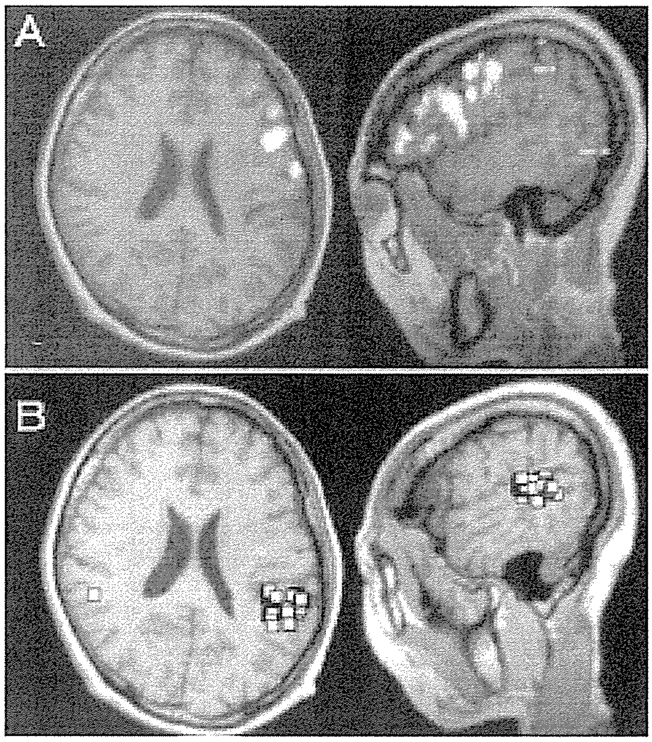

FIG. 2. Case 22. A left frontal lobe lesion in a 44-year-old, right-handed woman. A: Functional MR images obtained during a language task, showing activations mainly in the left MFG and dorsolateral PFC. B: Magnetoencephalography source localizations obtained during a language task, superimposed on MR images, showing dipole clusters in the left superior temporal region, including the SMG. The left and right hemispheres contained 93 and 19 dipoles, respectively.

follows: in the posterior part of the IFG (pars opecularis) and MFG in 12 patients, only in the MFG in six patients, and in the whole IFG in four patients. The dorsolateral PFC and supplementary motor area were bilaterally activated in 16 patients.

Magnetoencephalographic Profiles and Dipole Locations

All 22 patients were able to perform the MEG language task and demonstrated lexicosemantic responses peaking at approximately 400 msec after letter presentation (N400m). The N400m were predominantly observed in the MEG sensors covering the frontotemporal regions. Dipole clusters of the N400m were located in the superior temporal region, including the STG and MTG of the suspected dominant hemisphere in all 22 patients, in the SMG in 13 patients, and in the inferior temporal region (fusiform gyrus and ITG) in five patients (Fig. 1B and 2B). The results of the MEG language task showed that the left hemisphere was dominant for temporal lobe receptive-language function in 19 patients and the right hemisphere was dominant in three. The mean total numbers of dipoles in the suspected dominant and nondominant hemispheres (with SDs) were 92.0 ± 39.1 and 40.2 ± 25.8, respectively. The mean ratio (± SD) of the number of dipoles in the dominant hemisphere to the number in the nondominant hemisphere was 2.3 ± 1.8 (range 1.43–9.4).

The fMR imaging and MEG depicted the frontal expressive and temporal receptive language functions well and consistently identified the dominant hemisphere. The results of the noninvasive functional mapping were confirmed by results of the amobarbital test, that is, left-sided dominance in 19 patients and right-sided dominance in 3 patients. Demographic data on all the patients are shown in Table 1.

Arcuate Fasciculus Tractography

Although the AF is very difficult to locate on regular MR imaging sequences, the fractional anisotropy or color vector maps demonstrated the AF as a high-anisotropic or green (anterioposterior orientation) area in the frontotemporal white matter in all 22 patients (Fig. 3A and B). The tractography results were strongly supported by the results of the fMR imaging and MEG with language tasks (Fig. 3C and D). The area of activation on fMR imaging was usually greater than the size of the MEG dipole clusters in our previous studies.[9,10] We chose diameters of 25 and 30 mm for the seed and target spheres, respectively, thereby including more than 80% of the MEG dipoles and the pixels that were activated in the temporal and frontal language areas in the functional 3D images (Fig. 3E).

The AF was thus clearly distinguished from other subcortical connections, with little contamination (Fig. 3F).

TABLE 1

*Demographic data on 22 patients with lesions affecting the arcuate fascicles in the dominant hemisphere**

Case No.	Age (yrs), Sex	Handed-ness	Dominant Hemisphere fMRI	MEG	Wada Test	Lesion Location	Symptoms	Histological Findings
1	38, M	rt	lt	lt	lt	lt temporal	gen seizure	astrocytoma (Gr I)
2	37, F	lt	rt	rt	rt	rt temporal	gen seizure	astrocytoma (Gr II)
3	28, M	rt	lt	lt	lt	lt frontotemporal	mild rt hemiparesis	astrocytoma (Gr III)
4	37, F	rt	lt	lt	lt	lt frontal	gen seizure	astrocytoma (Gr II)
5	54, M	rt	lt	lt	lt	lt temporal	none	GBM
6	28, F	rt	lt	lt	lt	lt temporal	gen seizure	astrocytoma (Gr II)
7	32, F	rt	lt	lt	lt	lt frontal	mild rt hemiparesis & dysarthria	astrocytoma (Gr III)
8	45, M	rt	lt	lt	lt	lt frontal	mild rt hemiparesis	astrocytoma (Gr III)
9	43, F	rt	lt	lt	lt	lt frontal	gen seizure	astrocytoma (Gr II)
10	32, M	rt	lt	lt	lt	lt frontal	none	astrocytoma (Gr II)
11	43, M	rt	lt	lt	lt	lt frontal	gen seizure	astrocytoma (Gr III)
12	32, F	rt	lt	lt	lt	lt frontotemporal	none	astrocytoma (Gr II)
13	18, F	rt	lt	lt	lt	lt frontal	gen seizure	astrocytoma (Gr II)
14	38, M	rt	lt	lt	lt	lt frontal	gen seizure	astrocytoma (Gr II)
15	50, F	rt	lt	lt	lt	lt frontal	none	astrocytoma (Gr III)
16	45, F	rt	lt	lt	lt	lt temporal	mild sensory aphasia	GBM
17	44, F	rt	lt	lt	lt	lt frontal	gen seizure	astrocytoma (Gr II)
18	71, M	rt	lt	lt	lt	lt frontal	rt hemiparasis & dysarthria	GBM
19	22, F	rt	lt	lt	lt	lt frontal	mild rt hemiparesis	GBM
20	49, M	lt	rt	rt	rt	rt frontotemporal	gen seizure	astrocytoma (Gr II)
21	61, F	lt	rt	rt	rt	rt frontal	dysarthria & numbness in lt face	GBM
22	44, F	rt	lt	lt	lt	lt frontal	transient amnesia	astrocytoma (Gr II)

* gen = generalized; Gr = grade.

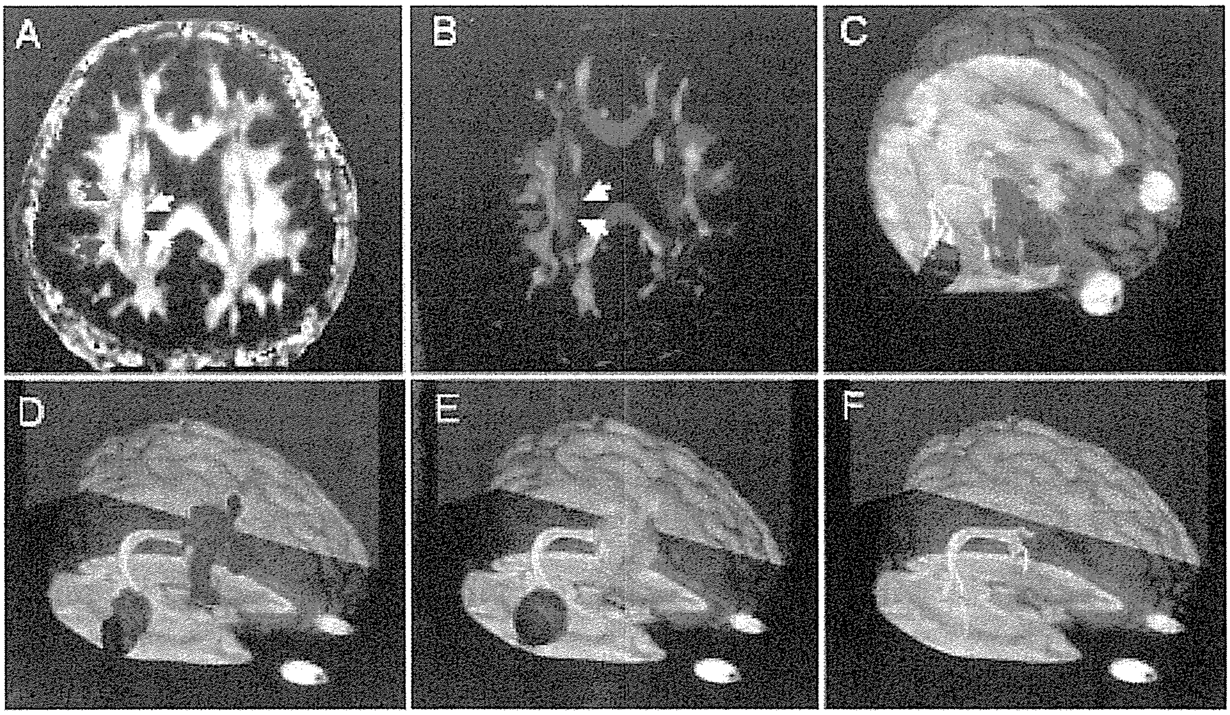

FIG. 3. Case 21. A: A fractional anisotropy map demonstrating higher anisotropic components, such as the AF *(red arrow)* and corticospinal tract *(white arrow)*, as white areas. B: A color vector map showing the fibers in the anteroposterior orientation, including the AF *(red arrow)* and corticospinal tract *(white arrow)*, which appear as green and blue areas, respectively. C and D: Three-dimensional reconstructions of functional information, including fMR imaging activation during a language task *(red)*, MEG dipoles from the MEG language task *(blue)* and results of AF tractography *(orange)*. E: Three-dimensional reconstruction of functional information showing the two regions of interest (seed and target points) for the AF tractography, which contain the frontal fMR imaging activation *(blue sphere)* and temporal MEG dipoles *(pink sphere)*. F: Results of AF tractography created by using the seed and target points and a threshold fractional anisotropy value of 0.16.

Regardless of whether the target was placed in the frontal-expressive or temporal-receptive language area, we obtained a reproducible AF profile. The mean fractional anisotropy value of all AF pixels was 0.17 ± 0.24. We, therefore, set a value of 0.16 as the appropriate threshold for extracting anisotropic components of the AF. The DT imaging–based tractography showed that the AF was medially compressed in five patients, inferiorly compressed in two, and partly involved by the lesions in two patients.

Cases of Awake Surgery

Awake surgery and subcortical stimulation were performed in two of the 22 cases. The symptom elicited by subcortical stimulation was consistent and highly reproducible in both cases.

Case 21

This 61-year-old, left-handed woman had suffered from dysarthria and numbness in her left lip for a month. Fluid-attenuated inversion-recovery MR imaging demonstrated a hyperintense 2-cm lesion mainly involving the right MFG (Fig. 4A). Functional MR imaging during verb generation demonstrated obvious activation in the posterior part of the right IFG and the inferior part of the MFG, which partly covered the tumor (Fig.1 A). On the MEG language task there were 127 dipoles in the right hemisphere and 37 in the left; the main dipole clusters were located in the right STG and MTG (Fig. 1B). The right hemispheric dominance, identified by the fMR image and MEG language tasks was confirmed by the Wada test. Because the tumor extended to the subcortical white matter in addition to involving parts of the MFG, it was important to clarify the spatial relationships between the eloquent structures and the lesion. The AF tractography was initiated from the seed point, including the area of activation on fMR imaging in the IFG, to the target point in the superior temporal region, and the U-shaped AF was visualized using an threshold fractional anisotropy value of 0.16 (Fig. 3).

During intraoperative cortical mapping, 10 mA of electrical current applied to the posterior part of the IFG and the inferior part of the MFG consistently caused speech arrest without oromotor seizure. Stimulation of the upper part of the MFG, however, elicited little dysarthria and no speech arrest (Fig. 5A and B). We therefore decided to perform a corticotomy in the upper part of the MFG, which covered the subcortical tumor. We removed the tumor carefully, observing whether subcortical stimulation caused language deficits. Although stimulation directly to the AF visualized on functional neuronavigation did not suppress spontaneous speech, it severely impaired naming acuity. During the subcortical stimulation, the patient could speak naturally, but failed to name all 15 pictures—that is, she experienced paranomia. The stimulus points related to paranomia were adjacent to the identified AF (Fig. 5). The resection was therefore stopped to preserve the language-related functions. We measured the minimum distance between the resection cavity and the identified AF by segmentation of signal intensity on isotropic postoperative DT images (Fig. 6A). Although the minimum distance was 1.2 mm and the AF seemed to be preserved on the DT imaging–based tractography, the patient suffered from transient but severe postoperative motor-dominant aphasia. The aphasia lasted for longer than 6 months and then gradually resolved. The histopathological diagnosis was GBM. One year after surgery, the patient's speech had deteriorated because of tumor recurrence and she was again experiencing motor-dominant aphasia.

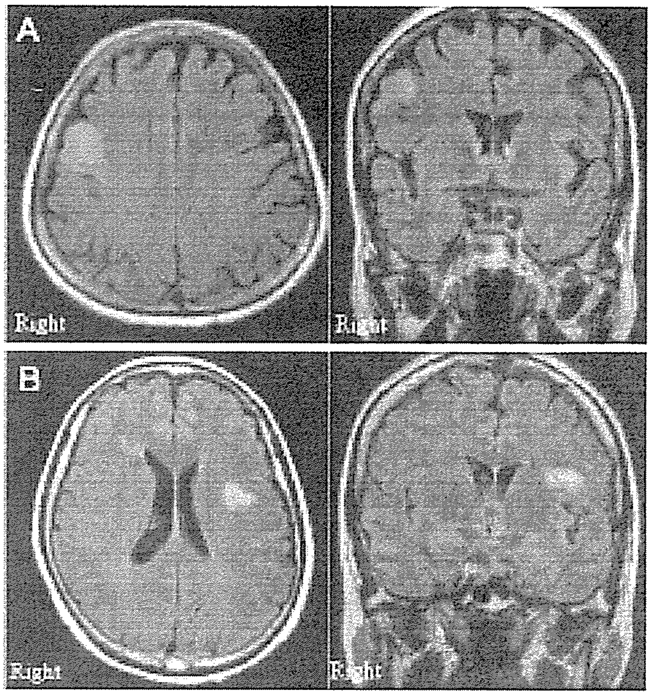

FIG. 4. Fluid-attenuated inversion-recovery MR images showing a hyperintense lesion in the right MFG of the patient in Case 21 (A) and in the left IFG and MFG of the patient in Case 22 (B). Hyperintense lesions suggest glial-origin tumors because of unclear tumor margins.

Case 22

This 44-year-old, right-handed woman with a suspected glial-origin lesion in the left frontal lobe (Fig. 4B) experienced transient amnesia. In the functional mapping studies, activation on fMR imaging was restricted to the left MFG and dorsolateral PFC, and MEG dipoles were concentrated in the left superior temporal region, including the SMG (Fig. 2A and B). We performed DT imaging–based tractography by using the functionally identified language centers, and we were able to visualize the AF and establish that it was partially involved by the tumor.

During awake surgery, speech arrest was elicited by cortical stimulation to the MFG, and we selected a transsulcal approach between the IFG and MFG. to reach the lesion. After partially removing the lesion, we found that subcortical stimulation to the AF at the bottom of the resection cavity caused paranomia without speech arrest. We stopped resection at this point on the basis of our experience in Case 21. The distance measured on the postoperative DT imaging was 5.4 mm. No neurological symptom was observed. The histopathological diagnosis was Grade II astrocytoma.

Discussion

There is continuous interest in the monitoring of lan-

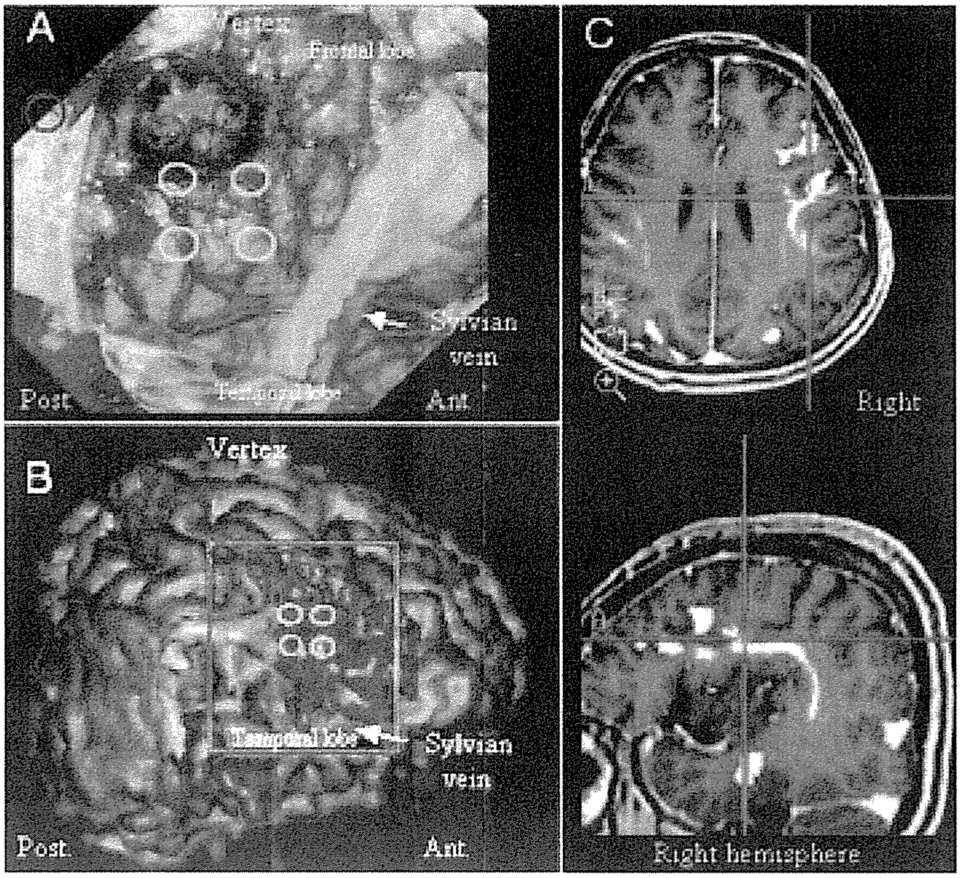

FIG. 5. Case 21. A: Photograph showing intraoperative findings. Cortical stimulation to the IFG and the inferior part of the MFG *(yellow circle)* and the primary motor cortex *(blue circle)* generated speech arrest and inhibition of voluntary hand movement, respectively. Subcortical stimulation to the bottom of the resection cavity *(red circle)* elicited paranomia without speech arrest. B: A 3D functional neuronavigation reconstruction of data from an MR image of the patient's entire head showing the activation on fMR imaging during the language task *(red)* as well as the AF *(yellow)* and MEG dipoles from the MEG language task *(blue)*. The *pink circle* and *blue square* indicate the corticotomy and the simulated operative window, respectively. Small *yellow, red, and blue circles* designate the stimulus points, which are the same as those in panel A. C: Two-dimensional MR images on the functional neuronavigation system demonstrating that resection reached the AF.

guage function during resection of tumors involving the frontotemporal regions. Awake surgery is the gold standard for direct monitoring of language functions, although this procedure entails certain risks related to anesthesia and requires that patients should be capable of cooperating during the operation. Electrical stimulation during awake surgery is also known to produce false-positive signs due to varying patient and stimulus conditions. In this study, DT imaging–based tractography with the seed and target points placed on functional 3D MR imaging, consistently visualized the AF in all 22 patients. In the two cases in which patients underwent awake surgery, stimulation to the gyri involving the areas identified on the fMR imaging language task evoked speech arrest, while subcortical stimulation to the AF consistently caused paranomia with no speech arrest. On the basis of the results of the subcortical mapping performed in Cases 21 and 22, we believe that the AF visualized on DT imaging–based tractography might be a real anatomical and functional structure.

Berman and colleagues and our group have recently reported the use of DT imaging–based tractography and intraoperative neurophysiological monitoring for the preservation of the corticospinal tract.[2,11] Furthermore, we added an electrophysiological validation of the visualized corticospinal tract using direct subcortical stimulation. We used five-train monopolar electrical stimuli for the subcortical mapping and showed that the motor evoked potentials were consistently observed when distances between the stimulus point and the visualized corticospinal tract were within 5 mm on the functional neuronavigation.[11] The combination of subcortical stimulation and functional neuronavigation provided excellent identification of the anatomical profiles of the corticospinal tract.

Excellent illustrations of the AF and optic radiation in healthy volunteers were recently obtained using virtual fiber dissection with standardization of normal control data.[3,4] This technique, however, is not applicable in pathological brain conditions. In the investigations reported to date, this technology has only been used for anatomical studies; the studies did not involve the direct assessment of functional connectivity.

Duffau and colleagues have suggested that direct subcor-

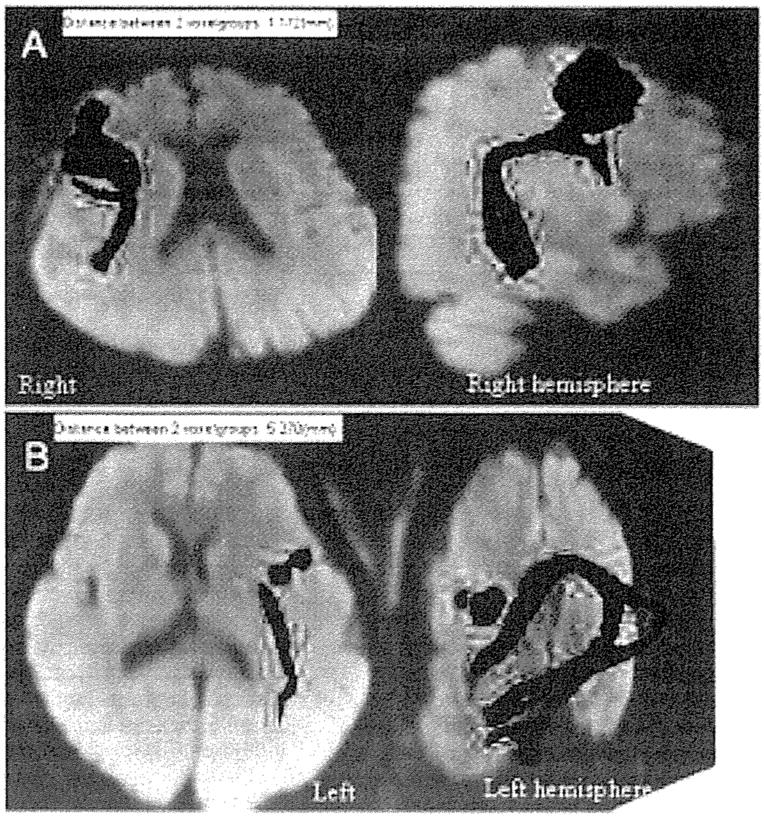

FIG. 6. Quantitative analysis of the distance between the resection cavity and the AF on isotropic images. A: The distance in Case 21 was 1.2 mm, and tumor resection caused transient but severe motor-dominant aphasia. B: The distance in Case 22 was 5.4 mm, and no neurological symptom was observed after resection.

tical stimulation offers the advantage of identifying the cortical and subcortical structures essential for language functions. In their studies, subcortical stimulation in the frontal lobe frequently caused semantic paraphasia.[7,8] Nevertheless, the subcortical stimulation procedure, including searching for optimal stimulus points and testing the several semantic tasks, requires the interruption of resection procedures, resulting in a longer operation time.

In the two cases in our study in which we performed intraoperative mapping, we found that speech arrest and paranomia were independently caused by the bipolar stimulation to the frontal cortex and AF, respectively. These dissociated impairments of expressive language functions were specifically produced by the alternate use of cortical and subcortical stimulations. The findings strongly suggested that suppression effects caused by subcortical stimulation to the AF spread over the whole language network, because there is probably little inhibitory system in the white matter. In addition, the distance between stimulus points and the visualized AF was 1.2 mm in Case 21 and 5.4 mm in 22. Because the patient in Case 22 did not experience postoperative neurological deterioration, we hypothesize that 6 mm might be a safe distance for resection, although we acknowledge that the small number of cases studied (two) limits the generalizability of our results.

We used two different modalities for noninvasive cortical mapping. Functional MR imaging has become popular for identifying hemispheric language dominance, and most investigators who have used this modality have found activations in the IFG and MFG during word generation and categorization tasks.[10,13,18]

Some researchers have focused on the correspondence between fMR imaging and cortical stimulation in the frontotemporal region and have reported speech arrest as a result of cortical stimulation to the frontal areas that showed activation during fMR imaging language tasks.[17,19] On the other hand, detection of the receptive language function by fMR imaging has been empirically more difficult than detection of expressive language function.[13,20]

Magnetoencephalography is another option that is highly complementary to fMR imaging. Cortical evoked potentials recorded by subdural electrodes have been reported to show responses at approximately 200 (early) and 400 (late) msec on the cortices of the left temporal base and the superior temporal gyrus after letter presentation.[16] The late potentials were observed mainly in the temporal region during experiments that required people to make decisions about visually presented words.[12] In our study, the late component sources in the periods between 250 and 600 msec were located mostly in the posterior parts of the temporal region. Using cortical stimulation, Simos and associates[21] have validated the locations of the MEG dipoles seen in the superior temporal region in association with language tasks, and they have shown excellent agreement between the mapping results of both techniques. Our method, using the results of fMR imaging and MEG, identified independent cortical centers of the frontal and temporal language functions and potential regions of interest for the AF tractography.

The fiber orientation depicted on DT imaging–based tractography reflects the average orientation of axonal fibers in each pixel and is susceptible to the extent of tissue heterogeneity. Within each pixel, a minor proportion of fibers always run in a different direction from the majority. Therefore, at present, DT imaging–based tractography can only provide gross anatomical information on major tracts in the white matter. For AF tractography, we acquired contiguous DT imaging slices with relatively thin slice thickness (3 mm) to increase the spatial resolution of the z axis to follow the curvature of the AF profile.

Conclusions

In the near future, several new techniques to improve DT imaging–based tractography should become available. These include high angular sampling of k-space, the interpolation or regularization of tensor fields, and global energy minimization for fiber tracking. The combination of these techniques should provide a powerful tool for preserving language-related functions in neurosurgery. Appropriate selections of the seed and target points determined by fMR imaging and MEG studies incorporating language tasks enable the elucidation of the real AF. Although the number of patients who underwent awake surgery in our study group is small, we did find that subcortical stimulation to the walls of the resection cavity consistently and efficiently caused semantic paranomia with no speech arrest. The electrophysiological validation in these patients supported the premise that DT imaging–based tractography can yield real functional information pertaining to the AF which can be valuable in neuroscience research as well as clinical practice. Studies of this kind will play an essential role in developing an understanding of the underlying semantic networks.

References

1. Basser PJ, Mattiello J, LeBihan D: MR diffusion tensor spectroscopy and imaging. **Biophys J 66:**259–267, 1994
2. Berman JI, Berger MS, Mukherjee P, Henry RG: Diffusion-tensor imaging-guided tracking of fibers of the pyramidal tract combined with intraoperative cortical stimulation mapping in patients with gliomas. **J Neurosurg 101:**66–72, 2004
3. Catani M, Jones DK, Donato R, ffytche DH: Occipito-temporal connections in the human brain. **Brain 126:**2093–2107, 2003
4. Catani M, Jones DK, ffytche DH: Perisylvian language networks of the human brain. **Ann Neurol 57:**8–16, 2004
5. Chen HM, Varshney PK: Mutual information-based CT-MR brain image registration using generalized partial volume joint histogram estimation. **IEEE Trans Med Imaging 22:**1111–1119, 2003
6. Duffau H: Intraoperative direct subcortical stimulation for identification of the internal capsule, combined with an image-guided stereotactic system during surgery for basal ganglia lesions. **Surg Neurol 53:**250–254, 2000
7. Duffau H, Capelle L, Sichez N, Denvil D, Lopes M, Sichez JP, et al: Intraoperative mapping of the subcortical language pathways using direct stimulations. An anatomo-functional study. **Brain 125:**199–214, 2002
8. Duffau H, Gatignol P, Mandonnet E, Peruzzi P, Tzourio-Mazoyer N, Capelle L: New insights into the anatomo-functional connectivity of the semantic system: a study using cortico-subcortical electrostimulations. **Brain 128:**797–810, 2005
9. Kamada K, Sawamura Y, Takeuchi F, Houkin K, Kawaguchi H, Iwasaki Y, et al: Gradual recovery from dyslexia and related serial magnetoencephalographic changes in the lexicosemantic centers after resection of a mesial temporal astrocytoma. Case report. **J Neurosurg 100:**1101–1106, 2004
10. Kamada K, Takeuchi F, Kuriki S, Todo T, Morita A, Sawamura Y: Dissociated expressive and receptive language functions on magnetoencephalography, functional magnetic resonance imaging, and amobarbital studies. Case report and review of the literature. **J Neurosurg 104:**598–607, 2006
11. Kamada K, Todo T, Masutani Y, Aoki S, Ino K, Takano T, et al: Combined use of tractography-integrated functional neuronavigation and direct fiber stimulation. **J Neurosurg 102:**664–672, 2005
12. Kutas M, Hillyard SA: Brain potentials during reading reflect word expectancy and semantic association. **Nature 307:**161–163, 1984
13. Lehéricy S, Cohen L, Bazin B, Samson S, Giacomini E, Rougetet R, et al: Functional MR evaluation of temporal and frontal language dominance compared with the Wada test. **Neurology 54:** 1625–1633, 2000
14. Masutani Y, Aoki S, Abe O, Hayashi N, Otomo K: MR diffusion tensor imaging: recent advance and new techniques for diffusion tensor visualization. **Eur J Radiol 46:**53–66, 2003
15. Masutani Y, Yoshikawa T, Aoki S, Ohtomo K, Sherbondy A, Napel S: EPI distortion correction for MR-DTI by using texture memory on graphics hardware. **Proc of CARS'03 (London):** 1315, 2003
16. Nobre AC, Allison T, McCarthy G: Word recognition in the human inferior temporal lobe. **Nature 372:**260–263, 1994
17. Roux FE, Boulanouar K, Lotterie JA, Mejdoubi M, LeSage JP, Berry I: Language functional magnetic resonance imaging in preoperative assessment of language areas: correlation with direct cortical stimulation. **Neurosurgery 52:**1335–1345, 2003
18. Rutten GJ, Ramsey NF, van Rijen PC, Alpherts WC, van Veelen CW: FMRI-determined language lateralization in patients with unilateral or mixed language dominance according to the Wada test. **Neuroimage 17:**447–460, 2002
19. Rutten GJ, Ramsey NF, van Rijen PC, Noordmans HJ, van Veelen CW: Development of a functional magnetic resonance imaging protocol for intraoperative localization of critical temporoparietal language areas. **Ann Neurol 51:**350–360, 2002
20. Rutten GJ, Ramsey NF, van Rijen PC, van Veelen CW: Reproducibility of fMRI-determined language lateralization in individual subjects. **Brain Lang 80:**421–437, 2002
21. Simos PG, Papanicolaou AC, Breier JI, Wheless JW, Constantinou JEC, Gormley WB, et al: Localization of language-specific cortex by using magnetic source imaging and electrical stimulation mapping. **J Neurosurg 91:**787–796, 1999

Manuscript received February 23, 2006.

Accepted in final form August 7, 2006.

This work was supported in part by the Japan Epilepsy Research Foundation; the Takeda Promotion of Science Foundation; Grant-In-Aid No.17591502 for scientific research from MEXT (the Japanese Ministry of Education, Culture, Sports, and Technology); a Research Grant from the Princess Takamatsu Cancer Research Fund; the Terumo Promotion of Science Foundation; the Brain Science Foundation; and Grant-In-Aid No. 18020010 for scientific research on priority areas (integrative brain research) from MEXT.

Address reprint requests to: Kyousuke Kamada, M.D., Department of Neurosurgery, Faculty of Medicine, The University of Tokyo, 7-3-1 Hongo, Bunkyo-ku, Tokyo 113-8655 Japan. email: kamady-k@umin.ac.jp.

EXPRESSIVE AND RECEPTIVE LANGUAGE AREAS DETERMINED BY A NON-INVASIVE RELIABLE METHOD USING FUNCTIONAL MAGNETIC RESONANCE IMAGING AND MAGNETOENCEPHALOGRAPHY

Kyousuke Kamada, M.D., Ph.D.
Department of Neurosurgery,
The University of Tokyo,
Tokyo, Japan

Yutaka Sawamura, M.D., Ph.D.
Department of Neurosurgery,
Hokkaido University,
Sapporo, Japan

Fumiya Takeuchi, Ph.D.
Research Institute for Electric Science,
Hokkaido University,
Sapporo, Japan

Shinya Kuriki, Ph.D.
Research Institute for Electronic Science,
Hokkaido University,
Sapporo, Japan

Kensuke Kawai, M.D., Ph.D.
Department of Neurosurgery,
The University of Tokyo,
Tokyo, Japan

Akio Morita, M.D., Ph.D.
Department of Neurosurgery,
The University of Tokyo,
Tokyo, Japan

Tomoki Todo, M.D., Ph.D.
Department of Neurosurgery,
The University of Tokyo,
Tokyo, Japan

Reprint requests:
Kyousuke Kamada, M.D., Ph.D., and
Tomoki Todo, M.D., Ph.D.,
Department of Neurosurgery,
The University of Tokyo,
7-3-1 Hongo, Bunkyo-ku,
Tokyo 113-8655 Japan.
Email: kamady-k@umin.ac.jp

Received, March 23, 2006.
Accepted, October 13, 2006.

It is known that functional magnetic resonance imaging (fMRI) and magnetoencephalography (MEG) are sensitive to the frontal and temporal language function, respectively. Therefore, we established combined use of fMRI and MEG to make reliable identification of the global language dominance in pathological brain conditions.

We investigated 117 patients with brain lesions whose language dominance was successfully confirmed by the Wada test. All patients were asked to generate verbs related to acoustically presented nouns (verb generation) for fMRI and to read three-letter words for fMRI and MEG.

fMRI typically showed prominent activations in the inferior and middle frontal gyri, whereas calculated dipoles on MEG typically clustered in the superior temporal region and the fusiform gyrus of the dominant hemisphere. A total of 87 patients were further analyzed using useful data from both the combined method and the Wada test. Remarkably, we observed a 100% match of the combined method results with the results of the Wada test, including two patients who showed expressive and receptive language areas dissociated into bilateral hemispheres.

The results demonstrate that this non-invasive and repeatable method is not only highly reliable in determining language dominance, but can also locate the expressive and receptive language areas separately. The method may be a potent alternative to invasive procedures of the Wada test and useful in treating patients with brain lesions.

Expressive language function, Functional magnetic resonance imaging, Language dominance, Magnetoencephalography, Receptive language function

Neurosurgery 60:296–306, 2007 DOI: 10.1227/01.NEU.0000249262.03451.0E www.neurosurgery-online.com

Brain asymmetries have been of considerable interest in neurology for more than a century. Based on clinicopathological studies, the "classical mode" of language organization consists of a frontal "expressive" area for planning and executing speech and writing, and a temporal "receptive" area for analysis and identification of linguistic sensory stimuli. This basic scheme of language functions has generally been accepted, with the assumption that both expressive and receptive functions dominantly exist in the same hemispheric side.

The Wada test has been considered the most reliable method to determine language dominance. According to one of the largest studies performed to date, 4 and 96% of right-handed subjects with chronic epilepsy have speech dominance in the right and left hemispheres, respectively (3). Furthermore, several studies suggested the possibility of atypical language representation in patients with chronic epilepsy (20–30%) (9, 28). However, the procedure of successive anesthetization of each hemisphere by intracarotid injections of sodium amobarbital requires catheterization and irradiation. Furthermore, the Wada test results can only demonstrate a relative distribution of language functions across the two hemispheres. More detailed information on localization of specified language functions within a hemisphere is important for understanding the language networks, as well as the treatment of brain lesions.

The use of functional magnetic resonance imaging (fMRI) has recently been developed to identify the hemisphere with language dominance. Most language fMRI studies have observed activations in the inferior frontal gyrus (IFG) and middle frontal gyrus (MFG) using tasks such as word generation and categorization (16, 24, 29). Detection of the receptive language area by fMRI has been reported to be more difficult than that of the expressive language function, and the use of listening or sentence comprehension tasks has resulted in visualization of only a few pixels in the temporoparietal region (8, 16, 25, 26). In addition, a fundamental limitation of an fMRI-based brain mapping is the varying degrees of regional hemodynamic responses under pathological brain conditions (7, 10, 15). Therefore, a clinical interpretation of localized activations on fMRI remains complicated and controversial.

Magnetoencephalography (MEG) reflects intracellular electric current flow in the brain and allows accurate localization of the current dipole sources. Dipoles of MEG deflections that peaked at approximately 400 milliseconds after word presentation (late responses) have been observed to localize in the temporoparietal regions. These late responses have been considered to be related to the receptive language function (19, 20). We have also observed dense dipole clusters of the semantic late responses in the superior temporal gyrus (STG), supramarginal gyrus (SmG), and fusiform gyrus (FuG) of the suspected dominant hemisphere (11, 12). Therefore, we sought to use MEG not only as an additional diagnostic tool for identifying the language dominance, but also to localize the receptive language center.

In the present study, we describe a non-invasive method to locate the expressive and receptive language areas by co-utilizing fMRI and MEG. The language dominance determined by our method matched the results from the Wada test with 100% accuracy. The usefulness of the method was well demonstrated, especially in those patients who showed dissociated expressive and receptive language functions. The data show that this method is highly reliable and may be useful in the management of patients with brain lesions as well as in studying normal brain functions.

METHODS

Patients

The functional brain mapping using fMRI (with the verb generation task) and MEG was performed in 117 patients with brain lesions since August 1999 (>7 yr) after this project was approved by the Institutional Committee for Ethics (*Table 1*). fMRI studies with the abstract/concrete (A/C) categorization task were also performed in 106 patients. Ninety-seven patients also underwent the Wada test to confirm the dominant cerebral hemisphere for language functions. Six patients showed negative Wada test results owing to the steal effect of a large arteriovenous malformation (AVM) or an overdose. The final analyses were performed in 87 patients (48 men, 39 women), who underwent Wada test, fMRI, and MEG investigations. The mean age (± standard deviation) was 43.6 ± 14.1 years. The Edinburgh Handedness Inventory was used to estimate the patients' handedness (18). A written informed consent was obtained from the patient or his/her family before participation in the study.

Magnetic Resonance Protocols

Anatomic magnetic resonance imaging (MRI) and fMRI were performed during the same session with a 1.5-T whole-body magnetic resonance scanner with echo-planar capabilities and a standard whole-head transmit-receiver coil (Siemens Vision, Erlangen, Germany). During the procedures, foam cushions were used to immobilize the head.

Language fMRI

The patients were instructed to respond to all language tasks silently. fMRI data was acquired with a T2-weighted echo-planar imaging sequence (echo time, 62 ms; repetition time, 114 ms; flip angle, 90 degrees; slice thickness, 4 mm; slice gap, 2 mm; field of view, 260 mm; matrix, 64 × 128; 14 slices). Each fMRI session consisted of three dummy scan volumes followed by three activation and four baseline (rest) periods. During each period, five echo-planar imaging volumes were collected, yielding a total of 38 imaging volumes and 2 minutes 32 seconds in measurement time for each session. fMRI data of language-related semantic responses were acquired as follows. All subjects were examined with two different lexical semantic language paradigms; verb generation by listening to nouns and A/C categorization by reading words. All words for semantic tasks were selected from common Japanese words listed in the electronic dictionary of the National Institute for Japanese Language.

Verb Generation Task

For the auditory stimuli (duration ranges were between 400 and 600 ms), common concrete nouns spoken by a native Japanese speaker with a flat intonation were recorded and digitized with a sampling rate of 44,000 Hz. A backward playback of the sound files (reference sounds) was used to eliminate the primary auditory activation during the rest periods with the same inter-stimuli intervals (1600–2400 ms) as the active periods. The auditory stimuli were delivered binaurally via two 5-m-long plastic tubes terminating at a headphone. The sound intensity was approximately 95 dB sound pressure level at the subject's ear. Subjects were instructed to silently generate a verb related to each presented noun during the active periods and passively listen to the reference sounds during the rest periods.

A/C Categorization Task

Visual stimuli were presented on a liquid crystal display monitor with a mirror above the head coil allowing the patients to see the stimuli. Words consisting of three *Kana* letters (Japanese phonetic symbols) were presented in a 300-millisecond exposure time with interstimuli intervals ranging from 2800 to 3200 milliseconds. Patients were instructed to categorize the presented word silently into "abstract" or "concrete" based on the

TABLE 1. Summary of patients' brain lesions types

fMRI with VG + MEG	44	39	18	6	4	6	117
fMRI with A/C	41	34	15	6	4	6	106
Amytal test	42	29	16	6	4	0	97
Final analyses	39	26	12	6	4	0	87

AVM, arteriovenous malformation; fMRI, functional magnetic resonance imaging; VG, verb generation task; MEG, magnetoencephalography; A/C, abstract/concrete categorization task.

nature of the word. During interval periods, patients passively viewed random dots of destructured *Kana* letters that were controlled to have the same luminance as the stimuli to eliminate primary visual responses.

Before scanning, all patients had a brief practice time, and the fMRI examinations were repeated for each task to confirm the reproducibility. After data acquisition, a motion detection program (MEDx; Medical Numerics, Sterling, VA) discarded fMRI sessions containing motion artifacts exceeding 25% of the pixel size. A Gaussian spatial filter (6 mm in half width) was applied, and functional activation maps were calculated by estimating the Z-scores between the rest and activation periods using Dr. View (Asahi Kasei, Tokyo, Japan). Pixels with Z-scores higher than 2.2 ($P < 0.05$) were considered to indicate real activation and were used for mapping. Image distortion of fMRI was corrected by maximizing the mutual information of the fMRI data sets and three-dimensional T1-weighted MRI (3D-MRI) scans of the patient's brain (morphing compensation). The result from each fMRI session was co-registered with the 3D-MRI by the Affine transformation (5). After total number of the activated pixels in the IFG and MEG were automatically counted, a patient was considered to have unilateral language dominance when hemispheric pixels of one hemisphere counted less than 70% of the other hemisphere. Otherwise, the language dominance was considered bilateral.

Language MEG

The MEG signals were recorded with a 204-channel biomagnetometer (VectorView; Neuromag, Helsinki, Finland) in a magnetically shielded room. To confirm the reproducibility, we acquired two data sets for each task by repeating the MEG recording on two different days. One hundred fifty nouns consisting of three *Kana* letters were visually presented with a 300-millisecond exposure time with interstimuli intervals ranging from 2800 to 3200 milliseconds. Patients were instructed to judge whether or not the presented word was "abstract" or "concrete" based on the nature of the word and to push a button with the index or middle finger (*Kana* reading task). Each epoch consisted of a 500-millisecond prestimulus baseline and a stimulus followed by a 1500-millisecond analysis period. Epochs with a reaction time exceeding 1200 milliseconds and MEG examinations with a successful task performance less than 70% were discarded.

One hundred fifty epochs of the magnetic signals were averaged and digitally filtered between 0.1 to 30 Hz. Significant MEG deflections were visually identified based on the square root mean fields of more than 10 sensors in the frontotemporal (FT) or temporo-occipital (TO) regions. Locations and dipole moments of equivalent current dipoles were calculated every 2 milliseconds from 250 to 600 milliseconds after the stimulus onsets using the single equivalent dipole and sphere head models. Only those dipoles of which the measured and the calculated field distributions showed a correlation value of more than 0.85 and confidence volumes less than 1000 mm^3 were used. To confirm the calculated results, the same MEG time sections were analyzed using a current density map (low-resolution tomography; LORETA, Curry, Neuroscan, and Compumedics USA, El Paso, TX). The coordinates of the MEG system were transformed into anatomic 3D-MRI scans by identifying external anatomic fiduciary markers (nasion, left/right preauricular points), and estimated dipoles were superimposed onto the 3D-MRI scans.

Dipoles located in the temporal region, including the STG, MTG, SmG, and FuG, were manually counted. A patient was considered to have unilateral language dominance when hemispheric dipoles of one hemisphere counted less than 70% of the other hemisphere. Otherwise, the language dominance was considered bilateral.

Determination of Language Dominance using fMRI and MEG

On the basis of the results of language fMRI and MEG, we determined language dominance for each patient. When the semantic activation in one side of the IFG and MFG was wider than that of the other side during the language fMRI tasks, a patient was considered to have unilateral dominance for the expressive language function. When one side of the temporal region included more MEG dipoles than the other during the language MEG task, we determined that a patient had laterality of the receptive language function.

The Wada Test

All patients received injections of amobarbital (100 mg in a 10% solution, Amytal; Eli Lilly and Co., Indianapolis, IN) through a catheter placed in the internal car otid artery. Language testing was performed during the observation period of maximal amobarbital action as indicated by contralateral brachial plegia. Patients were given the following tasks in the following order and up to four points were given, depending on the severity of the language disturbance: 0, no response; 1, meaningless utterance; 2, incorrect repetition or paraphasia; 3, self-correction; and 4, unimpaired.

The tasks were as follows:

1) Spontaneous counting. Patients were instructed to count, starting immediately before the amobarbital administration and continuously until the next task was given. If the patient could continue to count even after brachial plegia appeared, obvious speech arrest and no impairment indicate 0 and 4 points, respectively.
2) Letter reading. Patients were instructed to read aloud seven words consisting of three or four *Kana* letters. The maximum score was 28 points (seven items × four points).
3) Naming. Patients were asked to name aloud the five objects presented pictorially. The maximum score was 20 points (five items × four points).
4) Auditory comprehension. Patients were asked to carry out three simple tasks such as blinking eyes, opening the mouth, and raising the unparalyzed arm. The maximum score was 12 points (three items × four points).
5) Pointing objects. Patients were shown a picture with a set of four objects and were instructed to point to one chosen by the investigator (e.g., "Point to the cat."). The maximum score was 16 points (four items × four points).

Performance in Tasks 1 and 3 were considered to reflect the expressive language capabilities (maximum score, 24 points); performance in Tasks 2, 4, and 5 reflected receptive language functions (maximum score, 56 points).

RESULTS

Handedness and the Wada Test

Ninety-one patients (80 right-, eight left-, and three bilateral-handers) successfully underwent the Wada test. Language dominance was left, right, and bilateral hemispheres in 81, six, and four patients, respectively. The language dominance of the right-handed patients was left in 75 patients (93.8%), right in two patients (2.5%), and bilateral in three patients (including one patient with dissociated expression and receptive functions [3.8%]), respectively. For left-handed patients, four patients showed left and four showed right dominance. For both-handed patients, two showed left dominance and one bilateral (dissociated). These results were similar to those of previous reports on language dominance (3, 4).

For further analysis, we subdivided the subjects into groups with chronic epilepsy and with non-epilepsy. In the epilepsy group (n = 29), left, right, and bilateral dominance was 24 (82.8%), three (10.3%), and two (6.9%), respectively. In the non-epilepsy group (n = 62), left, right, and bilateral dominance was 57 (91.6%), four (6.4%), and one (1.6%), respectively.

fMRI with the Verb Generation Task

The verb generation task was designed to locate the expressive language area by fMRI. Among 117 patients who underwent the verb generation task, 100 patients (84.6%) completed the task and provided useful fMRI data. The results showed that the dominant hemisphere for the expressive language function was left, right, and bilateral in 90, eight, and two patients, respectively. In the epilepsy group (n = 34), left, right, and bilateral dominance was 29 (85.2%), three (8.8%), and two (8.5%), respectively. In the non-epilepsy group (n = 66), left, right, and bilateral dominance was 61 (92.4%), five (7.6%), and zero (0%), respectively. The activated regions on fMRI mainly involved the IFG and MFG, the lateral precG, AG, and the supplementary motor area (SMA) (*Figs. 1* and *2*).

In some patients, activations were observed in bilateral hemispheres. Except for two patients who showed bilateral dominance, the activations in the non-dominant hemisphere were restricted to MFG and precG and smaller in size, so the pixels did not reach a cluster significance (maximum values of Z-score, <2.2 or <10 pixels).

Compared with successful results of the Wada test, the successful rate of fMRI with the verb generation task was 90.1%. Seven patients with aphasia or dementia failed to complete the task. Three glioma patients with marked surrounding, four patients with brain ischemia and three patients with large arteriovenous malformations failed to exhibit significant activations in the frontal lobe (*Fig. 3*). These incomplete results are accounted for by the reported disadvantage of fMRI that data may be affected by the pathological changes of cerebral circulation (7, 10, 15).

fMRI with the A/C Categorization Task

The A/C categorization task was designed to locate the receptive language area by fMRI. Among 106 patients who performed the A/C categorization task, 71 (67.0%) completed the task and provided useful fMRI data. Compared with the verb generation task, the A/C categorization task more often activated wider areas in bilateral hemispheres (*Fig. 2*). Activations generally involved the bilateral frontal lobes, including the IFG, MFG, and precG, with laterality. The superior temporal regions, such as the STG and SmG, demonstrated activation spots in only 45% (n = 32) of the investigated patients, and the side predominance was not apparent in most cases. The fMRI data of the A/C categorization task were considered unsuitable to determine the receptive language areas and were not used for the final analyses.

Language MEG Profiles and Dipole Locations

The *Kana* reading task was designed to locate the receptive language area by MEG. The language MEG was performed in 117 patients, of whom 99 (85.4%) completed the task and provided useful data (*Figs. 1* and *2*). Results showed that the dominant hemisphere for the receptive language function was left, right, and bilateral in 85, 11, and three patients, respectively. In the epilepsy group (n = 31), left, right, and bilateral dominance was 26 (83.9%), three (9.7%), and two (6.5%), respectively. In the non-epilepsy group (n = 68), left, right, and bilateral dominance was 59 (86.8%), eight (11.8%), and one (1.5%), respectively.

Dipole clusters of late deflections localized mainly in the superior temporal region (STG, MTG, and SmG), and 60% of investigated patients also showed dipoles in the inferior tempo-

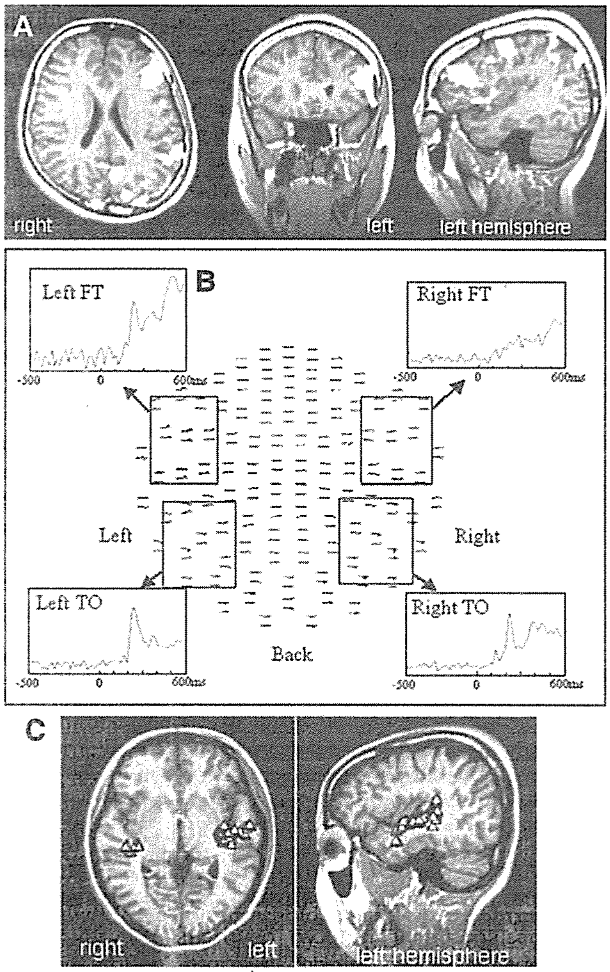

FIGURE 1. *A 24-year-old, right-handed man with epilepsy.* A, *fMRI with the verb generation task showing activations predominantly in the left IFG, MFG, PrecG, and parieto-occipital regions.* B, *square root mean field profiles of language MEG responses in the bilateral FT and TO regions. The left FT responses, peaking at 450 milliseconds, were markedly greater in amplitude than the right FT.* C, *source localization of the late deflections showing predominant dipole clusters (arrowheads) in the left superior temporal region. The left and right hemispheres contained 97 and 37 dipoles, respectively.*

ral region (FuG and inferior temporal gyrus). In 96 patients who showed unilateral language dominance, the total number of dipoles in the dominant versus non-dominant hemispheres was 124.1 ± 62.1 and 58 ± 30.9 (mean ± standard deviation), respectively. The ratio of the dipole number in the dominant hemisphere to the non-dominant hemisphere in each individual was 2.4 ± 1.7 (range, 1.43–14.4).

A typical result with all channels of MEG with the *Kana*-reading task is illustrated in *Figure 1*. Later deflections peaking at approximately 400 milliseconds were predominantly observed in the left FT. Bilateral TO regions demonstrated early deflections at approximately 200 milliseconds with short durations and little laterality. Estimated dipoles of the FT regions were densely accumulated in the left STG, MTG, and SmG (102 dipoles), whereas the right hemisphere showed fewer dipoles (54 dipoles) in the superior temporal region. This patient was thus determined to have receptive language dominance in the left temporal lobe.

The successful rate of language-MEG was 82.4%. Nine out of 39 epilepsy patients (23.1%) could not provide useful MEG data owing to artifacts from constant eye movements; the *Kana*-reading task was more difficult to complete than the verb generation task for patients with mental dysfunction. On the other hand, only one out of 18 AVM patients, owing to severe dyslexia, failed to provide useful MEG data, indicating that, in contrast to fMRI, MEG was not frequently affected by cerebral blood flow abnormalities (*Fig. 3*).

Combination of fMRI and MEG with Wada Test Verification

The verb generation task fMRI data depict expressive language areas well, but may be affected by cerebral blood flow abnormalities. The MEG results indicate receptive language areas well, but the task is rather complicated and may not be suited for patients with mental disorders. We sought to establish a non-invasive and reliable method to determine the laterality of language dominance by combining the advantages of these approaches. Furthermore, in terms of language functions, the results from fMRI and MEG can be integrated to locate expressive and receptive language areas and to provide reliable evidence whether or not there is dissociation. To verify the reliability of our method, 97 patients also underwent the Wada test.

Useful data from the method co-utilizing fMRI and MEG could be obtained from 87 out of 91 patients (95.6%). Remarkably, regarding language dominance, the results from the combination method matched the results of the Wada test in all 87 patients. Worth noting is that two patients (one with left temporal lobe epilepsy and the other with right insular astrocytoma) showed dissociated language areas using the combined method. The expressive language area was depicted in the left frontal lobe by fMRI, but the receptive language area was demonstrated in the right temporal lobe by MEG (*Fig. 4*). The Wada test results confirmed that both patients have language functions dissociated in the bilateral hemispheres. Among the 91 patients who underwent the Wada test, these were the only two patients in whom the Wada test detected dissociation of language functions.

In 12 epilepsy patients, the expressive and/or receptive language areas were electrophysiologically investigated via a subdural electrode implantation and the results were compared with those determined via the combined fMRI plus MEG method (*Fig. 5*). Out of eight patients who underwent cortical mapping for the expressive language area, all showed a speech arrest by electrical stimulation to the IFG and four to the MFG. All of the physiologically determined locations were confined within the areas depicted by the combined method. Out of six patients who received electrical stimuli to the temporal lobe,